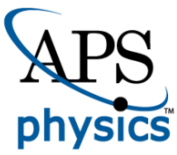

Two-Stage Ordering of Spins in Dipolar Spin Ice on the Kagome Lattice

Gia-Wei Chern, Paula Mellado, and O. Tchernyshyov

Phys. Rev. Lett. **106**, 207202 — Published 20 May 2011

DOI: 10.1103/PhysRevLett.106.207202

Two-stage ordering of spins in a dipolar spin ice on the kagome lattice

Gia-Wei Chern,[1] Paula Mellado,[2] and O. Tchernyshyov[3]

[1]*Department of Physics, University of Wisconsin, Madison, Wisconsin 53706, USA*
[2]*School of Engineering and Applied Sciences, Harvard University, Cambridge, Massachusetts 02138, USA*
[3]*Department of Physics and Astronomy, Johns Hopkins University, Baltimore, Maryland 21218, USA*

Spin ice, a peculiar thermal state of a frustrated ferromagnet on the pyrochlore lattice, has a finite entropy density and excitations carrying magnetic charge. By combining analytical arguments and Monte Carlo simulations, we show that spin ice on the two-dimensional kagome lattice orders in two stages. The intermediate phase has ordered magnetic charges and is separated from the paramagnetic phase by an Ising transition. The transition to the low-temperature phase is of the three-state Potts or Kosterlitz-Thouless type, depending on the presence of defects in charge order.

Frustrated magnets [1] attract attention of both theorists and experimentalists as models of strongly interacting systems with unusual ground states and elementary excitations. One of the recent surprises was a realization that elementary excitations in spin ice [2] are quasiparticles carrying magnetic charge [3]. Subsequent work [4] uncovered signatures of the magnetic monopoles in magnetization dynamics of spin ice. Spin ice is a frustrated ferromagnet discovered in the pyrochlore $Ho_2Ti_2O_7$, where magnetic Ho^{3+} ions form a network of corner-sharing tetrahedra [5]. The magnetic moments $\boldsymbol{\mu}_i = \sigma_i \mu \hat{\mathbf{e}}_i = \pm\mu\hat{\mathbf{e}}_i$ are forced to point along a $\langle 111\rangle$ axis $\hat{\mathbf{e}}_i$ by a strong crystal field. The easy-axis anisotropy makes the spins Ising-like, so that a microstate of this magnet can be described by Ising variables $\sigma_i = \pm 1$. The Hamiltonian of spin ice includes exchange interactions of strength J for pairs of nearest neighbors $\langle ij\rangle$ and dipolar interactions between all spins [2]:

$$H = -J\sum_{\langle ij\rangle}\sigma_i\sigma_j(\hat{\mathbf{e}}_i\cdot\hat{\mathbf{e}}_j) + \frac{Dr_{\rm nn}^3}{2}\sum_{i\neq j}\sigma_i\sigma_j\frac{(\hat{\mathbf{e}}_i\cdot\hat{\mathbf{e}}_j)-3(\hat{\mathbf{e}}_i\cdot\hat{\mathbf{r}}_{ij})(\hat{\mathbf{e}}_j\cdot\hat{\mathbf{r}}_{ij})}{|\mathbf{r}_i-\mathbf{r}_j|^3}, \quad (1)$$

where $D = (\mu_0/4\pi)\mu^2/r_{\rm nn}^3$ is a characteristic strength of dipolar coupling, $\mathbf{r}_i$ are spin locations, $\hat{\mathbf{r}}_{ij} = (\mathbf{r}_i - \mathbf{r}_j)/|\mathbf{r}_i - \mathbf{r}_j|$, and $r_{\rm nn}$ is the distance between nearest neighbors. In the absence of dipolar interactions, $D = 0$, and for ferromagnetic exchange, $J > 0$, the system is strongly frustrated because it is impossible to minimize the energy of every bond $\langle ij\rangle$. In a ground state, two spins point into every tetrahedron and two point out, which is reminiscent of proton positions in water ice, where every oxygen has two protons nearby and two farther away. This ice rule is satisfied by a macroscopically large number of microstates, so that both protons in water ice and magnetic moments in spin ice can remain disordered even at low temperatures [6].

Large magnetic moments ($\mu = 10\mu_B$ in $Ho_2Ti_2O_7$) make magnetic dipolar interactions between nearest neighbors comparable to exchange [7]. Together with the long-distance nature of dipolar interactions, the substantial value of D casts doubt on the usefulness of the short-range ($D = 0$) model of spin ice. Yet numerical simulations show that, even after the inclusion of dipolar interactions, energy differences between states obeying the ice rule remain numerically small—so small that magnetic order induced by the dipolar interactions is expected to occur only at a rather low temperature, $T \approx 0.13D$ [8–10]. The persistent near-degeneracy of ice ground states in the presence of dipolar interactions was clarified by Castelnovo *et al.* [3], who introduced a "dumbbell" version of spin ice, in which magnetic dipoles are stretched into bar magnets of length a such that their poles meet at the centers of tetrahedra. The energy of the resulting model can be represented as a Coulomb interaction of magnetic charges of the dumbbells, $q_i = \pm\mu/a$ [3]:

$$E(\{Q_i\}) = \sum_\alpha \frac{Q_\alpha^2}{2C} + \frac{\mu_0}{8\pi}\sum_{\alpha\neq\beta}\frac{Q_\alpha Q_\beta}{|\mathbf{r}_\alpha - \mathbf{r}_\beta|}. \quad (2)$$

In this expression, $Q_\alpha = \sum_{i\in\alpha} q_i$ is the sum of magnetic charges at the center of tetrahedron α. In a spin-ice state of the dumbbell model, every tetrahedron has two north and two south poles with a total magnetic charge $Q_\alpha = 0$, minimizing the first term in Eq. (2). As a result, no magnetic field will be generated and the magnetic dipolar energy is strictly zero. A partial cancellation occurs in the original model (1), making the Coulomb energy (2) a very good approximation. The charge of tetrahedron α, expressed in units of μ/a, is

$$Q_\alpha = \pm\sum_{i\in\alpha}\sigma_i, \quad (3)$$

with the plus sign for one sublattice of tetrahedra and minus for the other. Residual interactions, responsible for the formation of magnetic order, are weak and fall off quickly with the distance [3]. The resulting energy differences between states obeying the ice rule are only a small fraction of the dipolar energy scale D [9–11]. As the magnet is cooled down from a high-temperature paramagnetic state with completely uncorrelated spins, it first gradually enters the spin-ice regime at the crossover temperature $T \approx 2J_{\rm eff}$, where $J_{\rm eff} = J/3 + 5D/3$ is the effective interaction for nearest-neighbor Ising spins σ_i [2],

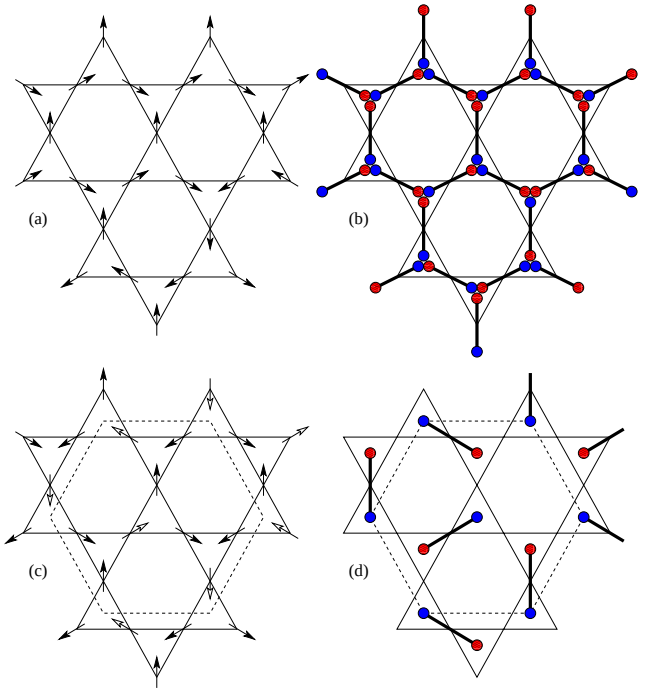

FIG. 1: Magnetic configurations of the dipolar kagome ice and their alternative representations. (a) A spin-ice microstate lacking spin order but possessing charge order. The latter is manifested in the dumbbell representation (b). (c) One of the ground states exhibiting the $\sqrt{3}\times\sqrt{3}$ magnetic order and its depiction in terms of dimers (d). The dashed line marks the magnetic unit cell.

and then undergoes a phase transition into a magnetically ordered state at $T \approx 0.13D$.

In this Letter, we discuss a related problem of dipolar spin ice on kagome, a two-dimensional lattice of corner-sharing triangles. Each spin is constrained to point along the line connecting the two triangles, Fig. 1(a). Possible ways of realizing such a system are discussed below. A short-range version of this model ($D = 0$, $J > 0$) was studied by Wills *et* al. [12].

At a first glance, the dipolar spin ice on kagome is very similar to its counterpart on the pyrochlore lattice and one might expect a similar sequence of transformations, namely a crossover to a correlated but disordered spin-ice state followed by a transition into a magnetically ordered phase. However, a closer look reveals the existence of an intermediate thermodynamic phase with ordered magnetic charges and disordered spins. To see this, note that the allowed values of magnetic charge (3) are even on a tetrahedron and odd on a triangle. Consequently, minimization of the first term in Eq. (2) yields $Q_\alpha = 0$ on the pyrochlore lattice and ± 1 on kagome. A microstate obeying the ice rule $Q_\alpha = \pm 1$, shown in Figs. 1(a) and (b), contains uncompensated charges that generate a magnetic field. To a first approximation, the system energy is given by the Coulomb term in (2). Nonzero values of magnetic charges result in substantial energy differences between states obeying the ice rule. The Coulomb energy is minimized when adjacent triangles carry charges of opposite signs. The charge-ordered states of the dipolar kagome ice are closely related to the ice states of the pyrochlore spin ice in a $\langle 111\rangle$ magnetic field [13]. The number of such states grows exponentially with the number of spins N. They are exactly degenerate in the dumbbell model. In the dipolar ice model (1), the degeneracy is lifted by small corrections to the Coulomb energy (2).

This hierarchy of energy scales suggests the following sequence of thermal transformations in the dipolar spin ice on kagome. As the magnet cools down from the high-temperature paramagnetic state with entropy per spin $s = \ln 2 = 0.693$, it gradually enters a spin-ice state with $s \approx (1/3)\ln(9/2) = 0.501$ [12]. At a temperature of the order of D, it will enter a distinct phase with ordered magnetic charges, where entropy density is reduced but remains nonzero, $s = 0.108$ per spin; the state is similar to that of the pyrochlore spin ice in a magnetic field along $\langle 111\rangle$ [13]. At an even lower temperature, the system will enter a spin-ordered state with zero entropy density. In contrast, spin ice with nearest-neighbor interactions only exhibits neither charge, nor spin order [12].

The above scenario of two-stage spin ordering is confirmed by our Monte Carlo simulations on the kagome dipolar ice model (1). A similar conclusion was reached independently in Ref. [14]. The specific heat $c(T)$ and entropy per spin $s(T)$ are shown in Fig. 2 for ferromagnetic exchange $J = 0.5D$, and antiferromagnetic $J = -2.67D$. In both cases, a broad peak in $c(T)$ signals a crossover from the paramagnetic regime to the spin-ice state. The latter is seen as a washed-out plateau in $s(T)$ near the characteristic spin-ice value $s \approx 0.501$. The crossover temperature $T \approx 2J_{\rm eff}$, where $J_{\rm eff} = J/2 + 7D/4$ on kagome. Two sharp peaks in $c(T)$ at lower temperatures mark the charge and spin-ordering phase transitions. In the antiferromagnetic case, $J = -2.67D$, the effective nearest-neighbor Ising coupling becomes small, $J_{\rm eff} = 0.415D$, so that the system is near the spin ice–antiferromagnet boundary, given approximately by the condition $J_{\rm eff} = 0$ [2]. This makes the spin-ice plateau indistinct, but the two phase transitions are clearly present.

We first discuss the details of the charge ordering transition and focus on the case of ferromagnetic exchange $J = 0.5D$. Monte Carlo simulations were performed with periodic boundary conditions and linear sizes up to $L = 36$, or $N = 3L^2 = 3888$ sites. Long-range dipolar interactions are summed over periodic copies up to a distance of $500L$. The temperature dependence of the staggered charge order parameter Q is shown in Fig. 3(a) for various system sizes. The existence of a continuous charge-ordering transition is evidenced by Fig. 3(b), where Binder's fourth-order cumulants of different L cross at $T_c \approx 0.267\,D$.

The Z_2 symmetry of the order parameter Q suggests

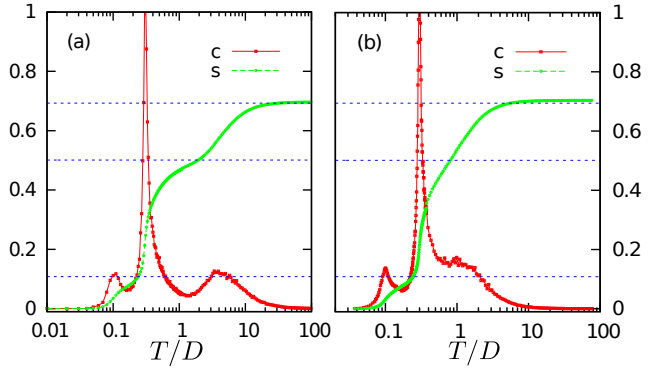

FIG. 2: Temperature dependence of the specific heat $c(T)$ and entropy per spin $s(T)$ of the dipolar spin ice (1) with (a) ferromagnetic exchange $J = 0.5D$ and (b) antiferromagnetic exchange $J = -2.67D$. The linear size of the system is $L = 12$. The dashed lines show levels of entropy $s = 0.693$ (Ising paramagnet), 0.501 (spin ice), and 0.108 (charge-ordered spin ice) per spin.

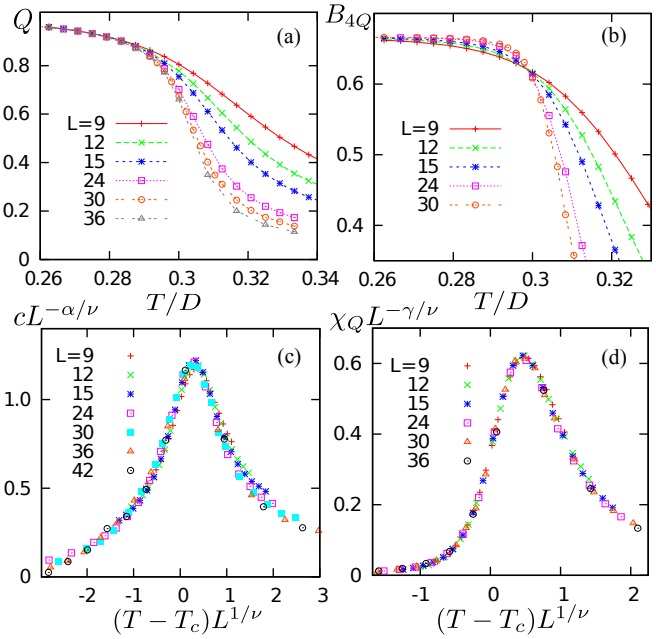

FIG. 3: Monte Carlo simulation of the charge-ordering transition in the spin-ice model (1). (a) and (b) show the temperature dependence of the staggered charge order parameter Q and Binder's fourth-order cumulant $B_{4Q} \equiv 1 - \langle Q^4\rangle/3\langle Q^2\rangle^2$. (c) and (d) show the scaling of specific heat c and charge-order susceptibility $\chi_Q = (\langle Q^2\rangle - \langle Q\rangle^2)/NT$ using critical exponents $\alpha = 0$, $\gamma = 7/4$ and $\nu = 1$ from the 2D Ising universality class.

that the charge-ordering transition is in the universality class of the Ising model. To verify this conjecture, we performed a finite-size scaling analysis and found excellent data collapse with the critical exponents of the 2D Ising universality class. Figs. 3(c) and (d) show the scaling behavior of the specific heat c and charge susceptibility χ_Q. In obtaining the scaled curves, we have subtracted a size-dependent background contribution from the specific-heat.

The spin order emerging on top of magnetic charge order is expected to be that of $\sqrt{3} \times \sqrt{3}$ type shown in Fig. 1(c), the same as in the short-range model with antiferromagnetic second-neighbor exchange [12]. This can be understood as follows. In a charge-ordered state every triangle has two majority spins pointing into (or out of) the triangle and a minority spin pointing the other way. Such states can be represented by dimer coverings of a honeycomb lattice, Fig. 1(d); the dimers indicate locations of minority spins. The energy of such a state is determined by the interactions between minority spins alone. To see that, picture a minority spin $-\boldsymbol{\mu}$ as a superposition of a majority spin $+\boldsymbol{\mu}$ and a minority spin of double strength $-2\boldsymbol{\mu}$; in this representation, majority spins form an inert background. We thus arrive at a model of dimers with point dipoles of strength 2μ directed along the dimers and towards triangles with positive charge. The interaction energy of two dimers depends on their mutual position. It is minimized by increasing the number of second neighbors (distance between centers $\sqrt{3}r_{\rm nn}$) and reducing the number of third neighbors ($2r_{\rm nn}$). The dimer configuration shown in Fig. 1(d) optimizes both. It is one of three states related to each other by lattice translations. The corresponding spin order is shown in Fig. 1(c). There are a total of 6 magnetic ground states related to each other by lattice translations and time reversal.

The symmetry-breaking pattern of the magnetic order described above suggests that the magnetic transition is in the universality class of the 2D three-state Potts model. However, Monte Carlo simulations of the dipolar ice model on systems up to $L = 36$ fail to turn up any evidence of the Potts critical behavior. The lack of a singularity in the specific heat [Fig. 4(a)] is consistent with a Kosterlitz–Thouless (KT) transition. This unexpected result can be understood by exploiting the previously mentioned mapping between ice states with perfect charge order and dimer coverings of the honeycomb lattice. The minimal dimer model consistent with the required magnetic order includes attraction between second-neighbor dimers v_2. We performed large-scale Monte Carlo simulations for the honeycomb dimer model using the worm algorithm [15]. As shown in Fig. 4(b), the transition into the $\sqrt{3} \times \sqrt{3}$ dimer order is indeed characterized by a KT transition similar to the case of dimer model on square lattice [16].

The presence of thermally excited defects in charge order spoils the mapping to dimer coverings. The counterpart of a charge defect in the honeycomb dimer model is a site with two dimers attached to it. We performed simulations with a finite fugacity $z = \exp(-\varepsilon/T)$ for such defects. The results for $\varepsilon = 2v_2$ are shown in Fig. 5. The

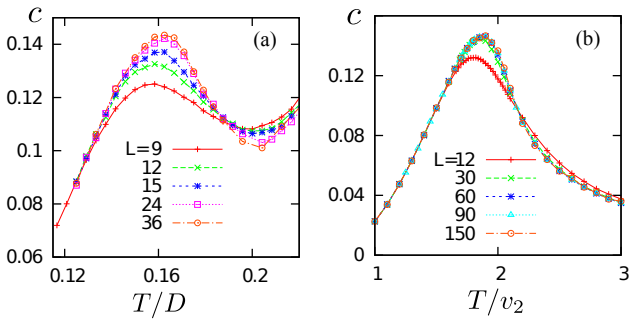

FIG. 4: Specific heat c as a function of temperature in Monte Carlo simulations of (a) dipolar spin ice model Eq. (1) on kagome, and (b) dimer model with attractive v_2 on honeycomb lattice. The peak of the specific heat curve corresponds to $\sqrt{3}\times\sqrt{3}$ magnetic and dimer ordering.

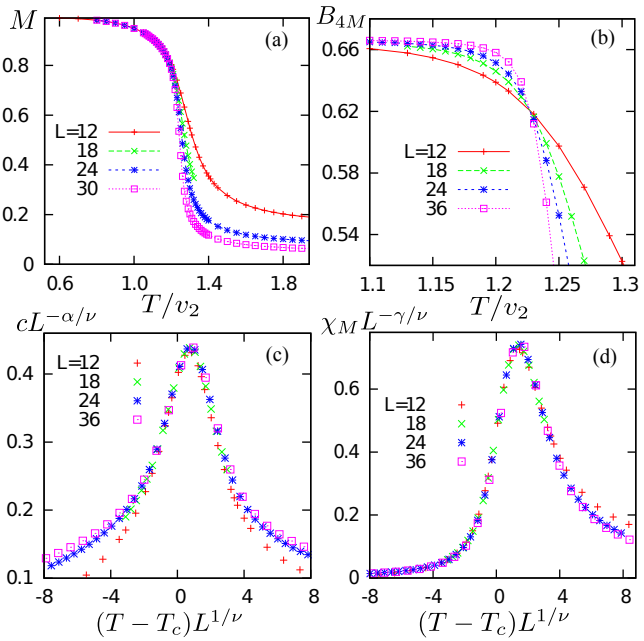

FIG. 5: Monte Carlo simulations of dimer ordering on a honeycomb lattice with a finite fugacity for charge defects. (a) and (b) show the temperature dependence of the magnetic order parameter M and Binder's fourth-order cumulant $B_{4M} = 1-\langle|M|^4\rangle/3\langle|M|^2\rangle^2$. (c) and (d) show the scaled specific heat c and magnetic susceptibility $\chi_M = (\langle|M|^2\rangle - |\langle M\rangle|^2)/NT$. The critical exponents of 2D three-state Potts model $\alpha = 1/3$, $\gamma = 13/9$, and $\nu = 5/6$ are used.

corresponding magnetic order parameter M is shown as a function of temperature in Fig. 5(a). Binder's cumulants cross at $T_m \approx 1.226\, v_2$ [Fig. 5(b)], indicating a continuous phase transition. Finite-size scaling with the critical exponents of the three-state Potts model gives excellent data collapse, Figs. 5(c) and (d).

These results illustrate the importance of charge defects for magnetic ordering. When the average separation between charge defects exceeds the system size, spin correlations decay algebraically with the distance, as expected from the dimer mapping. Consequently, one observes a KT-like magnetic transition for small systems of the dipolar ice model. The critical behavior characteristic of the three-state Potts universality only reveals itself for sufficiently large spin systems.

In summary, we presented a plausible scenario of a two-stage magnetic ordering in the dipolar spin ice on kagome. In contrast to spin ice on the pyrochlore lattice, this model has an intermediate phase distinguished by an Ising order of magnetic charges. The transition to the low-temperature phase is of the Kosterlitz-Thouless type if defects in charge order are absent and of the three-state Potts type if they are present. Kagome spin ice already exists as an artificial magnetic lattice [17, 18]. Although the energy scale of dipolar interactions in artificial ice greatly exceeds the room temperature, it may be possible to introduce thermal motion of spins by agitating them in a manner of granular systems [19].

We thank John Cumings, Roderich Moessner, and Peter Schiffer for valuable discussions. This work was supported by the NSF Award DMR-0348679 and by the DOE Award DE-FG02-08ER46544.

[1] *Introduction to Frustrated Magnetism,* C. Lacroix, P. Mendels, and F. Mila (eds.), Springer Series in Solid State Sciences, Vol. 164 (Springer, 2011).

[2] M. J. P. Gingras, in Ref. 1; arXiv:0903.2772.

[3] C. Castelnovo, R. Moessner, and S. L. Sondhi, Nature **451**, 42 (2008).

[4] L. D. C. Jaubert and P. C. W. Holdsworth, Nat. Phys. **5**, 258 (2009).

[5] M. J. Harris *et al.*, Phys. Rev. Lett. **79**, 2554 (1997).

[6] A. P. Ramirez *et al.*, Nature **399**, 333 (1999).

[7] B. C. den Hertog and M. J. P. Gingras, Phys. Rev. Lett. **84**, 3430 (2000).

[8] R. G. Melko, B. C. den Hertog, and M. J. P. Gingras, Phys. Rev. Lett. **87**, 067203 (2001).

[9] M. J. P. Gingras and B. C. den Hertog, Can. J. Phys. **79**, 1339 (2001); arXiv:cond-mat/0012275.

[10] S. V. Isakov, R. Moessner, and S. L. Sondhi, Phys. Rev. Lett. **95**, 217201 (2005).

[11] R. G. Melko and M. J. P. Gingras, J. Phys.: Condens. Matter **16**, R1277 (2004).

[12] A. S. Wills, R. Ballou, and C. Lacroix, Phys. Rev. B **66**, 144407 (2002).

[13] M. Udagawa, M. Ogata, and Z. Hiroi, J. Phys. Soc. Jpn. **71**, 2365 (2002).

[14] G. Möller and R. Moessner, Phys. Rev. B **80**, 140409(R) (2009).

[15] A. W. Sandvik and R. Moessner, Phys. Rev. B **73**, 144504 (2006).

[16] F. Alet *et al.*, Phys. Rev. E **74**, 041124 (2006).

[17] M. Tanaka *et al.*, Phys. Rev. B **73**, 052411 (2006).

[18] Y. Qi, T. Brintlinger, and J. Cumings, Phys. Rev. B **77**, 094418 (2008).

[19] X. Ke *et al.*, Phys. Rev. Lett. **101**, 037205 (2008).